Turkish Journal of Chemistry

Volume 39 | Number 5 Article 9

1-1-2015

Preparation and physicochemical characterizations of solid lipid nanoparticles containing DOTAP$^®$ for DNA delivery

GÜLAY BÜYÜKKÖROĞLU

EMİNE YASEMİN YAZAN

AYŞE FİLİZ ÖNER

Follow this and additional works at: https://journals.tubitak.gov.tr/chem

 Part of the Chemistry Commons

Recommended Citation

BÜYÜKKÖROĞLU, GÜLAY; YAZAN, EMİNE YASEMİN; and ÖNER, AYŞE FİLİZ (2015) "Preparation and physicochemical characterizations of solid lipid nanoparticles containing DOTAP$^®$ for DNA delivery," *Turkish Journal of Chemistry*: Vol. 39: No. 5, Article 9. https://doi.org/10.3906/kim-1412-40
Available at: https://journals.tubitak.gov.tr/chem/vol39/iss5/9

This Article is brought to you for free and open access by TÜBİTAK Academic Journals. It has been accepted for inclusion in Turkish Journal of Chemistry by an authorized editor of TÜBİTAK Academic Journals. For more information, please contact academic.publications@tubitak.gov.tr.

Turkish Journal of Chemistry

http://journals.tubitak.gov.tr/chem/

Research Article

Turk J Chem
(2015) 39: 1012 – 1024
© TÜBİTAK
doi:10.3906/kim-1412-40

Preparation and physicochemical characterizations of solid lipid nanoparticles containing DOTAP® for DNA delivery

Gülay BÜYÜKKÖROĞLU[1,*], Emine Yasemin YAZAN[2], Ayşe Filiz ÖNER[3]

[1]Department of Pharmaceutical Biotechnology, Faculty of Pharmacy, Anadolu University, Eskişehir, Turkey
[2]Department of Pharmaceutical Technology, Faculty of Pharmacy, Anadolu University, Eskişehir, Turkey
[3]Department of Pharmaceutical Biotechnology, Faculty of Pharmacy, Hacettepe University, Ankara, Turkey

Received: 17.12.2014 • **Accepted/Published Online:** 28.04.2015 • **Printed:** 30.10.2015

Abstract: The aim of this study was to prepare and evaluate stable cationic solid lipid nanoparticles (SLNs) as colloidal carriers for gene therapy. SLNs were mainly composed of three different biocompatible and biodegradable matrix lipids called tripalmitin, glyceryl dibehenate, and triglyceride, all containing the cationic lipid *N*-(1-(2,3-dioleoyloxy)propyl)-*N*,*N*,*N*-trimethylammonium (DOTAP®). Each of these SLNs were divided into three parts and characterized by applying different processes: Part I was autoclaved (121 °C, 15 min), Part II was lyophilized (5 mbar, –50 °C), and Part III was kept in its intact form. These parts were stored at 4 °C, 25 °C (room temp.), and 40 °C for short-term stability tests. The formulations were tested physically regarding the particle size and zeta potential. pUC18 plasmid DNA was used as the genetic material. Zeta potentials of all SLNs and pDNA-SLN complexes were determined to be highly positive (between +28.90 and +59.39). Crystallization processes of lipid matrices were characterized by X-ray diffractometry and differential scanning calorimetry. pDNA binding ability of SLNs and the stability of pDNA-SLN complexes with DNase I enzyme were also determined by gel electrophoresis. It was determined that all formulations became positively charged with DOTAP®. They were able to bind DNA and were partially protective against enzyme degradation. Although additional studies are necessary, this study reveals the promising potential of this gene delivery system for gene therapy.

Key words: Cationic solid lipid nanoparticles, DOTAP®, plasmid DNA, gene delivery, colloidal carriers, preparation, characterization, stability, SLN

1. Introduction

The establishment of gene therapy may be achieved by designing sophisticated gene delivery systems.[1] The goal of gene therapy is to treat diseases by delivering DNA or genes into defective cells. For this purpose, viral and nonviral gene carriers are being investigated to protect DNA and to aid in its cellular uptake.[2]

Viral vectors are currently the most efficient systems for the transfection of foreign DNA into living cells. However, they also have some disadvantages.[1,3,4] Viral vectors have the risk of oncogenicity, inducing immune responses and difficulties in industrial validation and upscaling.[5,6] In recent years, considerable interest has focused on the use of cationic compounds such as polyethylenimine (PEI)[3] and 1,2-dioleoyl-3-trimethylammonium-propane (DOTAP®) for the development of nonviral carrier systems. Complexes of DNA with PEI and with DOTAP® were reported to display a high transfection efficiency in cell cultures.[7]

*Correspondence: gbuyukko@anadolu.edu.tr

Gene transfer mediated by cationic lipid/DNA complexes (lipoplexes) and cationic polymer/DNA complexes (polyplexes) has been efficiently accomplished both in vitro and in vivo.[3,8] In vivo gene transfer is usually less efficient than in vitro gene transfer and it is not well predicted by in vitro results. The first and still most commonly used cationic lipid in lipoplex formulations is DOTAP, a monovalent positively charged nonnatural lipid that exhibits low in vivo toxicity.[9,10]

The mechanism of association of cationic lipids with plasmid DNA is mediated by a variety of physical interactions. The main mechanism is the ionic interaction between positively charged lipid head groups and negatively charged DNA phosphates,[5,11] which results in the formation of DNA complexes or lipoplexes. Lipoplexes are usually formulated with an excess amount of positive charge in order to mediate the interaction with the cell membranes, which carry a net negative charge.[5,10,12]

Cationic solid lipid nanoparticles (SLNs) were introduced as a nonviral transfection vehicle by Olbrich et al.[13,14] SLNs are an alternative drug delivery system to emulsions, liposomes, and polymeric nanoparticles.[15] Like emulsions and liposomes, SLNs consist of physiologically well-tolerated ingredients that have already been approved for pharmaceutical purposes in humans.[16] SLNs can be produced without the use of solvents that are potentially toxic and large-scale production is even possible.[15,17] Good storage stability and the possibility of steam sterilization and lyophilization are some of the advantages of SLN systems.[18] When a SLN system is produced with a cationic lipid, the resulting particles consist of a lipid core that presents cationic lipids on its surface and the cationic components are likely to be organized in raft-like monolayers, which allow the interaction between the modified SLN surface and DNA.[5,19]

The aim of this study was to compare the physical properties of different SLN formulations incorporating a cationic lipid to attach pDNA. For this purpose, three SLN formulations were formulated using three different matrix lipids including DOTAP to load pDNA and were evaluated with regard to their physical properties and stability features as a gene delivery system.

2. Results and discussion

High-energy input such as elevated production temperature, high stirring rate, long emulsification time, and/or strong ultrasound power is required to breakdown the droplets into nanometer range.[16,20] In our study, filtered and autoclaved SLNs displayed narrow size distributions and considerably small particle sizes (Table 1). During sterilization by autoclaving, the high temperature presumably led to an oil-in-water microemulsion formation due to phase inversion phenomena and probably affected the size of the nanodroplets.[21,22] After sterilization with an autoclave, increases in the average diameter and polydispersity index (PI) were observed only in the GSLN formulation.

After freeze-drying, slight increases in particle size and PI were observed for all SLNs. Particularly CSLN showed higher PI values, which was probably due to the presence of nanoparticle aggregates. The growth in the particle dimensions of lyophilized SLNs after resuspending systems comes from the effect on the structure of the crystal during freezing,[18] the formation of aggregate, and the fact that these aggregates cannot be redispersed completely.[17] Maintaining the average diameter and PI after redispersion of freeze-dried SLNs may be possible by incorporating a high percentage of surfactant and cryoprotectors.[21,23] In this situation, the main problem in the resuspended formulations is the high concentration of the surfactant and the cryoprotective.[24] The addition of cryoprotective to the formulations being prepared may cause the change of particle surface load, osmolality, and pH.[18] As the effects of ambient conditions on the formulations were researched comparatively, these substances were not added in order not to add a parameter that was different from other formulations and not to change the content of the formulation.

Table 1. Composition, mean particle sizes, and zeta potentials of the SLNs.

SLNs	Composition (% w/w)			Autoclaving process	Lyophilization	Particle size (nm) ± SE	PI	Zeta potential (mV) ± SE
	Lipid (4%)	Span85/Tween 80 (4%)	DOTAP (0.35%)					
DSLN	Dynasan® 116	2.4/1.6	+	—	—	180.3 ± 0.8	0.298	48.92 ± 0.6
$DSLN_O$	Dynasan® 116	2.4/1.6	+	+	—	176.9 ± 0.6	0.287	48.21 ± 0.3
$DSLN_L$	Dynasan® 116	2.4/1.6	+	—	+	680.2 ± 0.6	0.734	49.13 ± 0.2
GSLN	Gelucire® 33/01	2.4/1.6	+	—	—	166.8 ± 0.7	0.263	58.22 ± 0.4
$GSLN_O$	Gelucire® 33/01	2.4/1.6	+	+	—	185.3 ± 0.6	0.360	56.90 ± 0.5
$GSLN_L$	Gelucire® 33/01	2.4/1.6	+	—	+	664.2 ± 0.9	0.599	59.39 ± 0.6
CSLN	Compritol® ATO888	2.4/1.6	+	—	—	297.2 ± 0.6	0.483	35.91 ± 0.5
$CSLN_O$	Compritol® ATO888	2.4/1.6	+	+	—	218.0 ± 0.7	0.371	34.57 ± 0.2
$CSLN_L$	Compritol® ATO888	2.4/1.6	+	—	+	614.7 ± 0.7	1.000	28.89 ± 0.3

N = 3; PI: polydispersity index; SE: standard error.

Under all storage conditions, the stability of the formulations was satisfactory for the investigated parameters; the particle diameters and PIs showed a negligible degree of change within a few nanometers during a 9-month period ($P \geq 0.05$).

The surface charges determined by zeta potential measurements were measured to be highly positive, between +28.90 and +59.39 (Table 1). In general, lipid nanoparticles are negatively charged on the surface.[25] Although the amount of DOTAP added to the formulations was same, this variation seen in zeta potential depends on lipid matrices. Zeta potentials of DOTAP-free formulations were found as –21 ± 0.12 for Gelucire 33/01, –23 ± 0.14 for Dynasan®116, and –28 ± 0.10 for Compritol®ATO888. The attainment of different zeta potential with DOTAP used in the same ratio was based on this difference in lipids. Additionally, the temperature applied for Compritol ATO888 was the highest temperature (85 °C) and the effect of this temperature used for the formulation conditions on DOTAP may have decreased the efficiency of DOTAP.

Elevated temperatures are known to decrease the zeta potentials and increase the instability of the formulations. It was reported that the zeta potentials of the SLN formulations decrease after autoclave sterilization.[22,26] In our study, a slight decrease in zeta potentials of SLN formulations was detected after autoclaving ($P \geq 0.05$).

During the first 3 months, decrease in zeta potentials of all SLNs was not significant under all storage conditions ($P \geq 0.05$). A significant decrease was noted ($P \leq 0.01$) after a 9-month storage period, but zeta potential values still remained at a level sufficient enough to keep the particles stable against aggregation as determined by particle size analysis.

GSLNs showed the highest zeta potential and pDNA binding ability when compared to the CSLNs. On the other hand, zeta potential of GSLNs increased with the increasing amount of SLNs in pDNA-SLN complexes. pDNA complexes with DSLN or CSLN at the ratios of 1:10 and 1:50 were compared and no significant increase ($P \geq 0.05$) was found with the increasing amount of SLNs (Figure 1).

Differential scanning calorimetry (DSC) gives an insight into melting and recrystallization behaviors of crystalline materials like lipid nanoparticles.[27] All lipids and SLNs were analyzed by DSC to investigate their crystallinity. The DSC curves of lipids, lipid-DOTAP mixture, and lyophilized SLNs are given in Figures 2A–C and Figure 3, respectively. DOTAP did not show a sharp endothermic peak on the thermograms and similar behavior was also observed in X-ray studies. This suggests that DOTAP was not in the crystalline state. In order to see the behavior of DOTAP in lipid matrices, DSC analyses were performed after mixing the lipids and DOTAP at the temperatures used for SLN preparation [73 °C (Figure 2A), 45 °C (Figure 2B), 85 °C (Figure 2C)] and cooling down. Melting point, enthalpy, and crystallinity values of the lipids are demonstrated in Table 2.

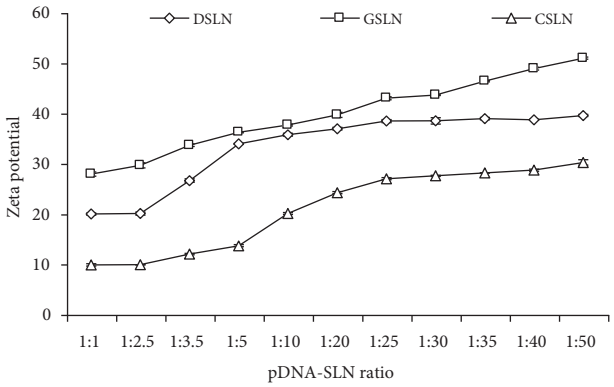

Figure 1. Zeta potentials of pDNA-SLN complexes.

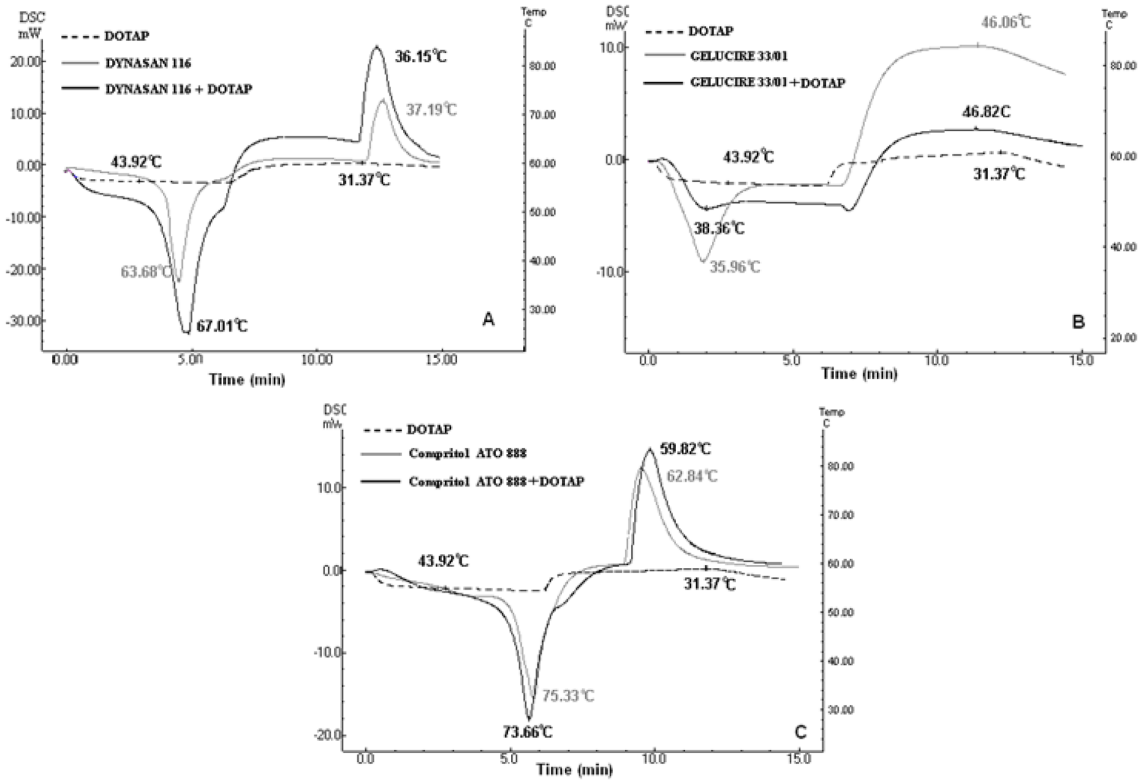

Figure 2. DSC thermograms of lipids and lipid-DOTAP mixtures.

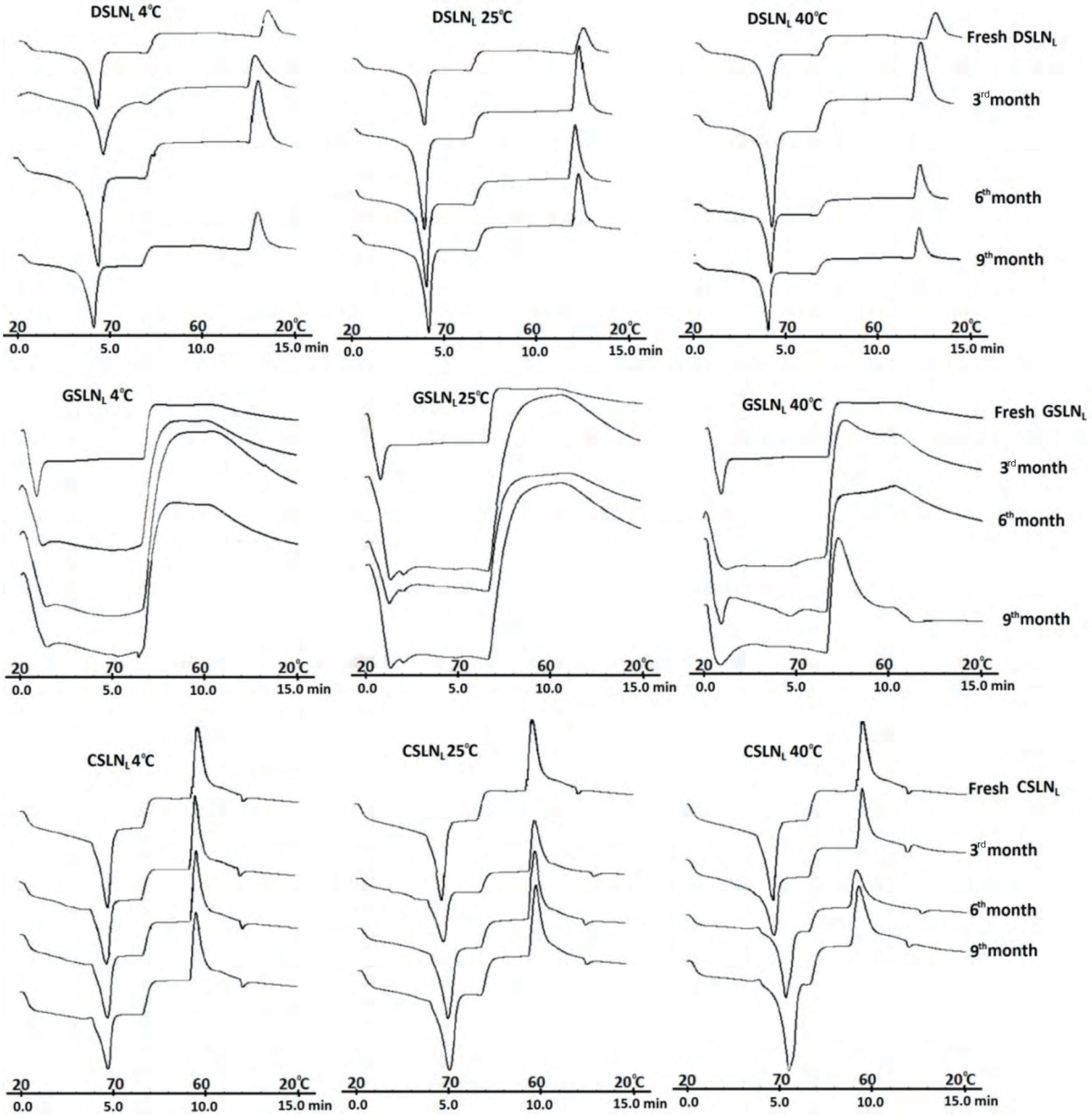

Figure 3. DSC curves of lyophilized SLNs stored at different conditions.

Table 2. Melting points, enthalpies, and crystallinities of lipid matrices.

	Lipid matrix	Melting point (°C)	Energy (J g^{-1})	Recrystallization point (°C)	Energy (J g^{-1})
1st heating	Dynasan 116	62.58	250.95	37.72	–162.74
	Gelucire 33/01	38.69	47.40	42.96	–91.61
	Compritol ATO888	73.56	63.91	61.09	–98.82
2nd heating	Dynasan 116	63.68	149.82	37.19	–88.21
	Gelucire 33/01	35.96	33.50	46.06	–16.32
	Compritol ATO888	75.33	160.40	62.84	–104.05

Melting points of filtered and autoclaved DSLNs increased with time (data not shown). This may be explained by the small particle sizes of the crystals.[27,28] The small particle size and therefore the high surface area, and also being in an energetically suboptimal state, may lead to a decrease in crystallization point.[21,27,29,30]

Triglycerides are known to crystallize mainly in three polymorphic forms, from α via β' to β. Increased melting point showed that the lipid was transformed from β' form to β form and an increase in the crystallization of the particles occurred. DSC curves of lyophilized DSLN (stored at 4 °C) indicated presence of an unstable (α) modification of the lipid at lower temperatures.[21,29,30] Appropriate storage condition was determined to be room temperature by comparing melting points of $DSLN_L$ samples stored under different conditions.

On the DSC thermograms of autoclaved and filtered GSLN samples, no sharp peaks were detected; however, endothermic and exothermic peaks were observed on the thermograms of $GSLN_L$ samples. At the end of 3 months, a shoulder peak was observed close to the principal peak, which gives a hint as to polymorphism.[28,31] No loss in typical peaks or no appearances of new peaks were recorded upon DSC analyses. This indicates that there was no interaction or incompatibility between the formulations prepared.[30] However, the thermogram of $GSLN_L$ stored at 40 °C showed a new peak after 9 months. The DSC analyses revealed that the storage condition of 4 °C was optimum for $GSLN_L$.

During the storage of CSLNs, increased tendency for recrystallization and gelling was observed. Gelled systems have much higher crystallinity values (100%–130%), indicating that the whole fat fraction is solid. Hence, it is possible to attribute the crystallinity changes to the energetic changes.[21,30] DSC measurements over a period of 3 months of autoclaved and filtered CSLNs stored at all storage conditions showed a continuous increase in the melting point close to the melting point of Compritol- DOTAP mixture (data not shown). At the end of 3 months, increase in the melting point and recrystallinity of CSLN stored at 40 °C was observed to be higher than that of those stored at 4 °C and room temperature. In addition, CSLN stored at 40 °C showed polymorphism at the end of 3 months. The appropriate storage condition for CSLN was determined to be 4 °C.

In order to examine the crystallinity of lipids and their lyophilized formulations with or without DOTAP, wide-angle X-ray studies were performed (Figures 4A–4D and 5A–5C), and thus the effect of DOTAP on the physical properties of lipids was investigated. DOTAP and Gelucire 33/01 were not in crystalline form (Figures 4A and 4B) in contrast to Compritol ATO888 (Figure 4C) and Dynasan 116 (Figure 4D). Dynasan 116 showed sharp peaks at angles of 16.24, 19.06, 22.78, and 23.74; these characteristic peaks, except the first peak, were observed in DSLN and $DSLN_L$ refraction profiles (Figure 5A). Sharp peaks of Compritol ATO888 were found in the refraction profiles of both CSLN and $CSLN_L$ at angles of 21.10 and 23.40 (Figure 5B). Degrees of crystallinity were compared on the basis of peak intensity, in which Dynasan 116 and Compritol ATO888 were found to have higher degrees than their formulations, which may be attributed to the effects of DOTAP or surfactants.

X-ray analysis of Gelucire 33/01 showed an amorphous state and two small peaks at angles of 20.78 and 23.07. These peaks did not appear in the profiles of GSLN; however, a secondary peak with low intensity appeared at the same angle in $GSLN_L$ (Figure 5C). The results obtained showed that DOTAP enhanced the maintenance of the crystalline form of Gelucire 33/01 in SLNs.

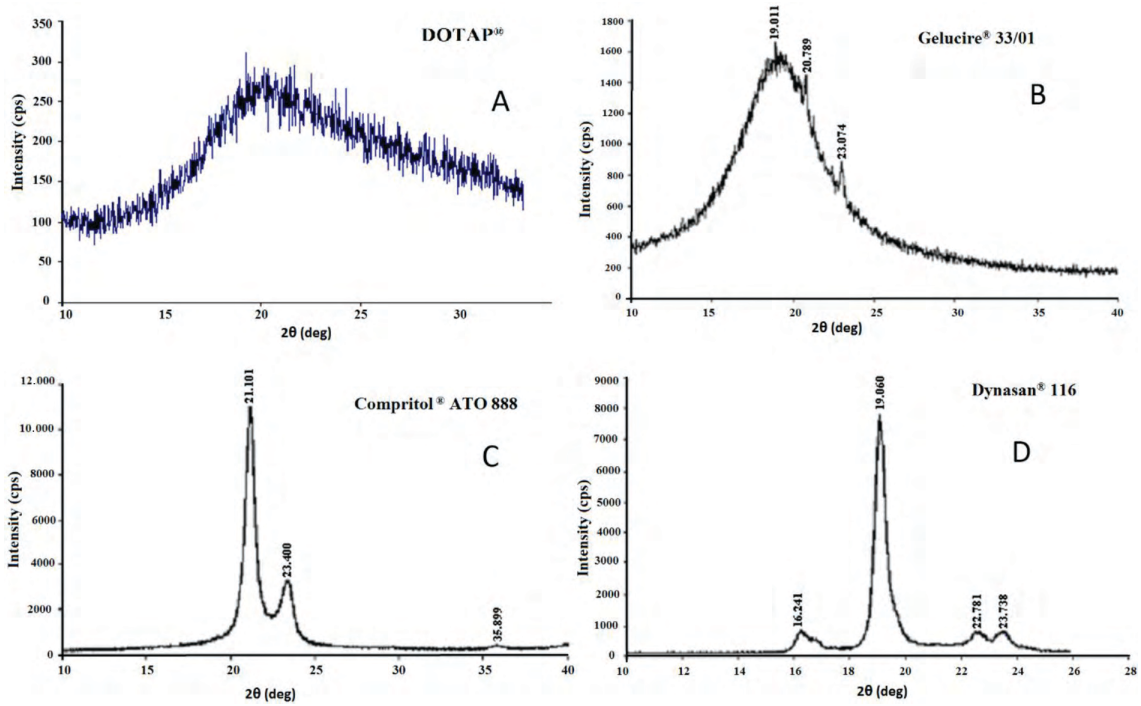

Figure 4. X-ray diffraction patterns of lipid matrices.

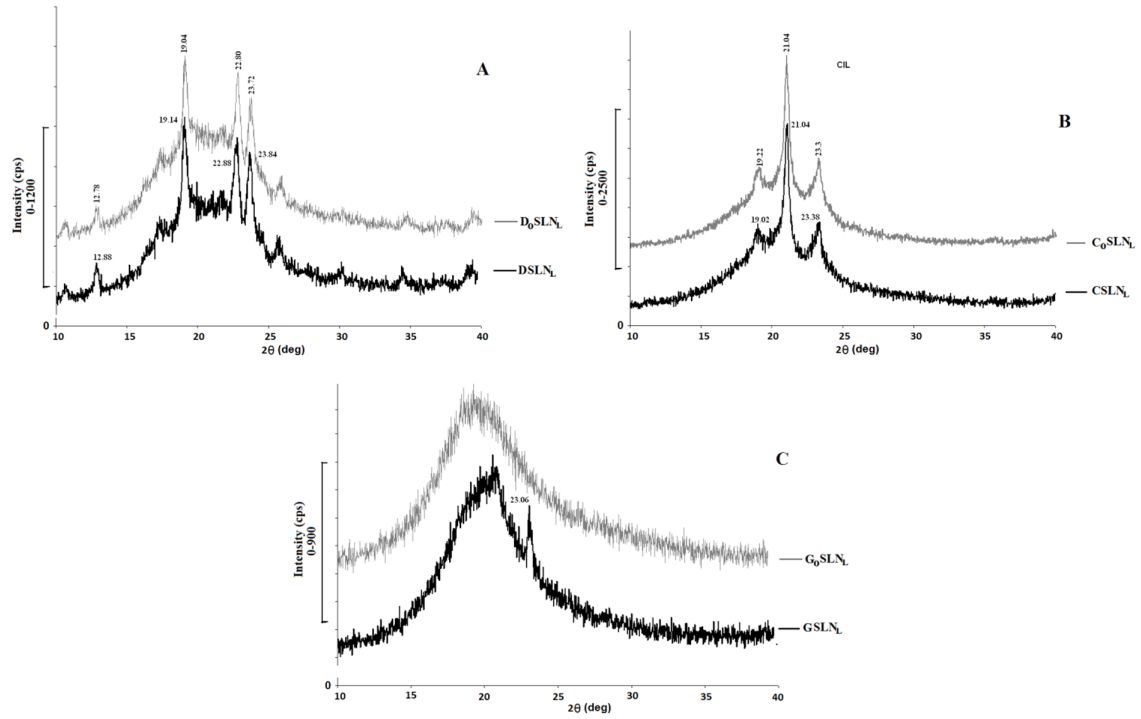

Figure 5. X-ray diffraction patterns of lyophilized SLNs. D_0SLNL: lyophilized SLN prepared with Dynasan 116 without DOTAP; C_0SLN_L: lyophilized SLN prepared with Compritol ATO888 without DOTAP; G_0SLN_L: lyophilized SLN prepared with Gelucire 33/01 without DOTAP, $DSLN_L$: lyophilized SLN prepared with Dynasan 116; $CSLN_L$: lyophilized SLN prepared with Compritol ATO888; $GSLN_L$: lyophilized SLN prepared with Gelucire 33/01.

In the comparison of X-ray diffraction patterns of lipids with the SLN formulations, overlapped peaks were detected in similar 2θ angles. These data verified that there was no difference in the crystal form of the materials due to the production parameters and use of DOTAP.

Retarded DNA bands on the agarose gels were observed as an indication of complex formation. Complete binding of pDNA with DOTAP and SLNs was confirmed by the absence of free DNA bonds on the gel images (Figures 6A–6G). Ten milligrams of DOTAP was weighed for 3 separate microtubes by heating to 43 °C, 73 °C, and 85 °C in order to determine the effect of formulation conditions on DOTAP. After this heating process, DOTAP was dispersed by vortex within 50 μL of distilled water in a tube and autoclaved. The complexation of these dispersions with DNA was compared with DOTAP, which was dispersed without heating. While the complexation rate of pDNA-DOTAP without heating was found as 1:10 (Figure 6A), it was found between 1:12 and 1:14 after heating (Figures 6B–6D) and as 1:16 after autoclaving (Figures 6E–6G). It was determined that the binding rate of DOTAP to DNA decreased depending on the temperature. However, heating to formulation temperatures was more effective than autoclaving temperature in decreasing the DNA binding ability of DOTAP.

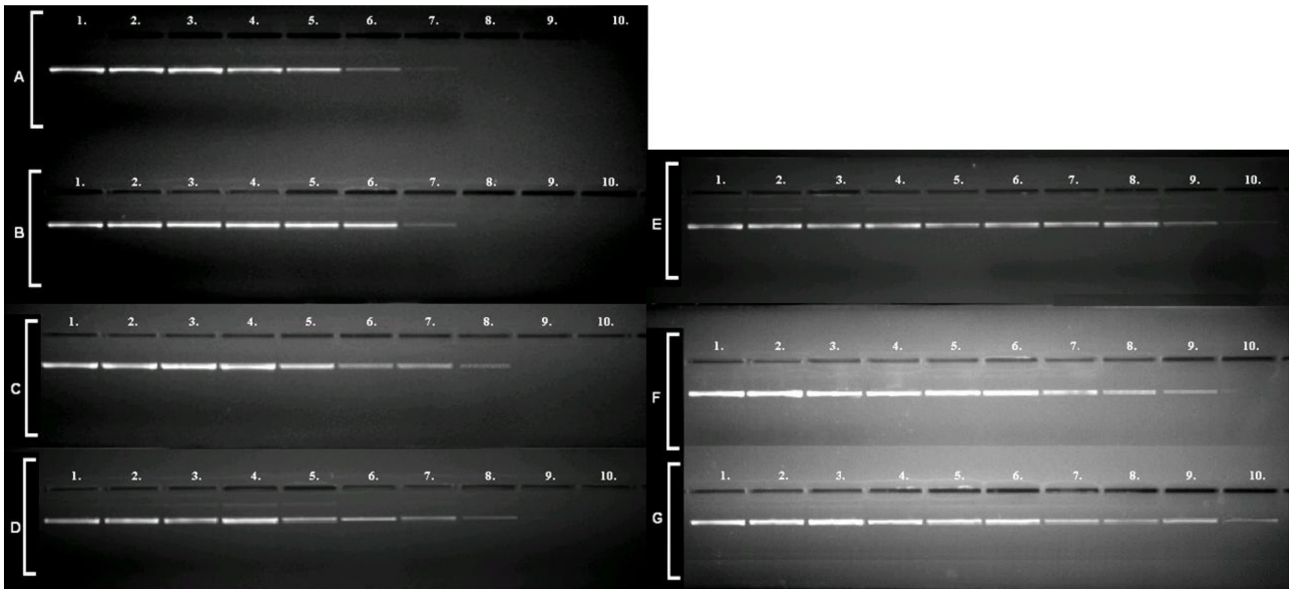

Figure 6. Agarose gel electrophoresis of mixtures of pDNA with DOTAP. Lines from left: pDNA only, pDNA:DOTAP mixtures with ratios (w/w) of 1:1, 1: 2, 1:4, 1:6, 1:8, 1:10, 1:12, 1:14, and 1:16. A) DOTAP dispersed in water, B) heating of DOTAP to 43 °C, C) heating to 43 °C and autoclaving of DOTAP, D) heating to 73 °C and autoclaving of DOTAP, E) heating to 73 °C and autoclaving of DOTAP, F) heating of DOTAP to 85 °C, G) heating to 85 °C and autoclaving of DOTAP.

pDNA binding abilities of filtered, lyophilized, and autoclaved SLNs were evaluated by using agarose gel electrophoresis (Figures 7A–7I). The results showed that filtered DSLN at a ratio of 1:4 was sufficient to bind the complete pDNA (Figure 7A).

DNA is a flexible polymeric molecule, exhibiting a wide range of conformations including open circular and supercoiled forms, and many studies indicated the formation of DNA-lipid complexes whose lamellar or columnar inverted-hexagonal structures depend upon the lipid composition and the cationic lipid-DNA ratio.[32–34] In the complexes, conformational changes of the DNA were anticipated on the basis of high positive charge density[35] and reduced relative humidity of the charged lipid bilayer.[36] DNA conformation changes were observed at a

DOTAP/DNA ratio of >1.0 by mixing DNA with liposomes containing the cationic lipid DOTAP or a 1/1 (mole ratio) mixture of DOTAP and DOPE. This phenomenon was described by Zuidam et al.[27]

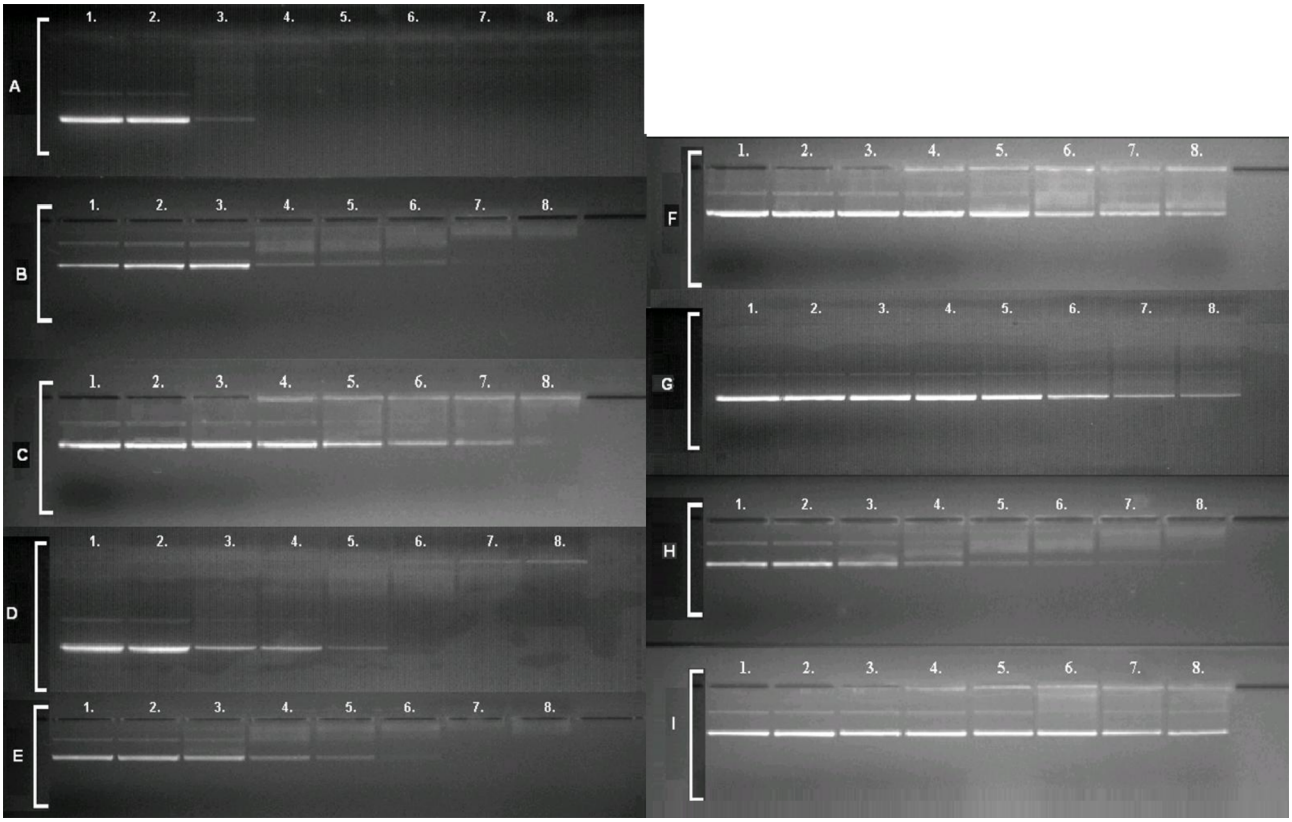

Figure 7. Agarose gel electrophoresis of mixtures of pDNA with filtered, lyophilized, and autoclaved SLNs. Lines from left: pDNA only (2 μg), pDNA:SLN complexes with ratios (w/w) of 1:1, 1: 2, 1:3, 1:4, 1:5, 1:6, and 1:7. A) DSLN, B) GSLN, C) CSLN, D) $DSLN_L$, **E)** $GSLN_L$, F) $CSLN_L$, G) $DSLN_O$, H) $GSLN_O$, and I) $CSLN_O$.

In this study, conformational changes of pDNA were observed on gels with filtered (Figures 7A–7C), lyophilized (Figures 7D–7F), and autoclaved (Figures 7G–7I) pDNA-SLNs complexes. Additional DNA bands to the bands of supercoiled and open circular forms of DNA were seen.

pDNA binding ability of CSLN was observed to be the weakest in comparison to the similar ratios of pDNA-DSLN and pDNA-GSLN. Consequently, the most efficient SLN for binding pDNA was found to be DSLN among the filtered SLNs, while GSLN was the most efficient among the lyophilized and autoclaved SLNs. pDNA binding ability of filtered DSLN was better than that of the lyophilized and autoclaved GSLN.

In therapeutic gene applications, the protection of pDNA from degrading enzymes is a critical factor for efficient gene delivery in vivo. Besides delivery purposes, a proper DNA carrier system must also protect DNA from nuclease attack.[7,37] In this study, we examined nuclease stability of the SLN-pDNA complexes against DNase I in vitro. SLN formulations were incubated with DNase I enzyme and pDNA recovered by using three different extraction methods. In all conditions, pDNA could be protected from total breakdown and remained highly intact, as seen in Figure 8. Conformation of pDNA changed, but smear formation was negligible when compared to naked pDNA (line 2), which was completely digested with an equal amount of DNAse I (line 3).

Conformational changes from supercoiled to open circular form might have resulted from either enzyme effect or extraction procedure. Changes in pDNA were detected during the extraction procedures without the presence of DNase I. According to the images seen in Figure 8, GSLN (lines 10 and 11) and CSLN (lines 13 and 14) formulations seem to protect pDNA against DNase I enzyme better than DSLN (lines 7 and 8) and Escort^T II (lines 5 and 6) do.

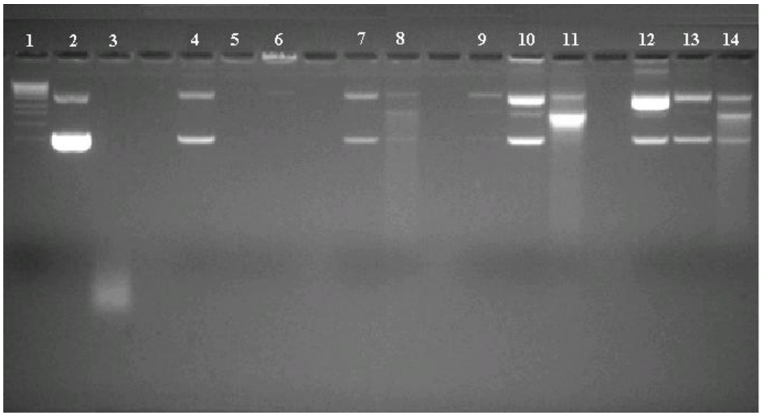

Figure 8. Stability of pDNA-SLN complexes in the existence of DNase I enzyme. Line 1: molecular weight marker (10 μg), line 2: pDNA only (4 μg), line 3: pDNA and DNase I enzyme (4 μg/4 U), line 4: pDNA only (4 μg), line 5: pDNA-Escort^T II (4 μg:16 μg), line 6: pDNA-Escort^T II and DNase I enzyme (4 μg:16 μg and 4 U), line 7: pDNA-DSLN (4 μg:40 μg), line 8: pDNA-DSLN and DNase I enzyme (4 μg:40 μg and 4 U). Extraction method I was used at lines 4–8. Line 9: pDNA only (4 μg), line 10: pDNA-GSLN (4 μg:40 μg), line 11: pDNA-GSLN and DNase I enzyme (4 μg:40 μg and 4 U). Extraction method II was used at lines 9–11. Line 12: pDNA only (4 μg), line 13: pDNA-CSLN (4 μg:40 μg), line 14: pDNA:CSLN and DNase I enzyme (4 μg:40 μg and 4 U). Extraction method III was used at lines 12–14.

3. Experimental

3.1. Materials

Tripalmitin (Dynasan 116) was supplied by Condea (Witten, Germany), and glyceryl dibehenate (Compritol ATO888) and triglyceride (hemi-synthetic triglyceride consisting of saturated fatty acids-C8-C18; Gelucire 33/01) were from Gattefossé (Nanterre, France). Cationic lipid N-(1-(2,3-dioleoyloxy)propyl)-N,N,N-trimethylammonium (DOTAP); the surfactants polyoxyethylene-20-sorbitan monooleate (Tween 80) and sorbitan trioleate (Span85®); and N-(2-hydroxyethyl)piperazino-N$'$-(2-ethanesulfonic acid) (HEPES) were purchased from Sigma Aldrich Chemicals (Germany). pUC18 plasmid DNA and DNase I enzyme were supplied by Fermentas (Lithuania).

3.2. Preparation of cationic SLNs

SLNs containing the cationic lipid DOTAP were produced by using an oil-in-water emulsification technique.[23] Dynasan 116 (DSLN), Compritol ATO888 (CSLN), and Gelucire 33/01 (GSLN), each containing DOTAP, were melted at about 10 °C above the melting point of each lipid and added to the hot aqueous surfactant solutions that were heated to same degree as lipids. Names and ratios of prepared formulations are shown in Table 1. The molten lipids were dispersed in the hot surfactant solutions by high-speed stirring (9500 rpm) using an Ultra

Turrax (IKA T-25, USA) type homogenizer.[38] All hot dispersions were filtered through a 0.2-μm nonpyrogenic filter (Schleicher & Schuell, Germany). Following filtration, each dispersion was divided into three portions. The first part was autoclaved (121 °C, 15 min), the second was lyophilized (5 mbar, –50 °C), and the third was kept in its intact form. The aliquots were stored for short-term stability tests at 4 °C, 40 °C, and room temperature (25 °C).

3.3. Preparation of pDNA-SLN complexes

pDNA was diluted to a final concentration of 1 μg/10 μL in 25 mM HEPES. Different amounts of SLNs were added to the tubes containing pDNA dispersion and incubated for 10 min at room temperature for complex formation at different ratios (1:1, 1:2.5, 1:3.5, 1:5, 1:10, 1:20, 1:25, 1:30, 1:35, 1:40, and 1:50) to maintain adsorption of negatively charged pDNA on positively charged particles.

3.4. Particle size and zeta potential

Mean diameter of the bulk population and the particle distribution via the PI of SLNs and pDNA-SLN complexes were analyzed by a Zetasizer NanoZS (Malvern Instruments, UK). Zeta potential was determined using the same equipment. Distilled water with a conductivity value of 50 μS/cm was adjusted using sodium chloride (0.1 N) at pH 7.4 and used in zeta potential analyses. Electrostatic mobility was converted to zeta potential using the Helmholtz–Smoluchowski equation.

For this purpose, 30 μL of the SLNs and pDNA-SLN complexes were dispersed in 1 mL of this distilled water and particle size, PI, and zeta potentials were measured.

3.5. DSC measurements

In order to determine the degree of crystallinity of the particle dispersion, DSC was used (DSC 60, Shimadzu, Japan). The heating rate was 10 °C/min between 25 °C and 90 °C, and then cooling down to 25 °C was performed with a cooling rate of 10 °C/min. The rate of crystallinity was estimated by comparison of the melting enthalpy/g of the bulk material with the melting enthalpy/g of the dispersion. Five milligrams of solid bulk material and 10 mg of dispersion were accurately weighed into aluminum pans, which were then sealed. An empty pan was used as a reference. Analyses were performed under nitrogen gas flow.

3.6. X-ray diffraction

X-ray diffraction pattern of each of the lipids (DOTAP, Dynasan 116, Compritol ATO888, and Gelucire 33/01) and all of the SLNs with or without DOTAP were recorded by using an X-ray diffractometer (Rigaku Rint 2200, Japan) at a range of 4–40 °C, using 40 kV voltage, 30 mA current, and 2° min^{-1} scanning rate.

3.7. Interaction of pDNA with DOTAP and SLNs

The effects of formulation conditions on the binding of pDNA to DOTAP were evaluated to determine the interaction between pDNA and DOTAP. Different ratios of pDNA-DOTAP (μg/μg) complexes were prepared and loaded on an agarose gel and visualized by 1.5% ethidium bromide staining for 2 h at 25 V. Images were obtained using Kodak Image Station 440 CF.

DSLN, GSLN, and CSLN were categorized as filtered, autoclaved, and lyophilized SLNs and binding rates of each SLN with pDNA were determined. Lyophilized SLNs were resuspended in 500 μL of autoclaved distilled water (pH 7.4).

pDNA was diluted in 25 mM HEPES (pH 7.4) to yield a final concentration of 1 μg 10 μL^{-1}. pDNA-SLN complexes were prepared at ratios (w/w) of 1:1, 1:2, 1:3, 1:4, 1:5, 1:6, and 1:7 and subjected to agarose gel electrophoresis.

3.8. Protection of pDNA-SLN complexes from DNase I digestion

Naked pDNA, pDNA-SLNs, and pDNA-Escort II complexes were incubated with 4 KU (Kunitz unit) of DNase I enzyme and the stability of pDNA in the complexes was investigated. DNA was recovered from complexes using 3 different extraction methods after incubation. In these methods, only solvents for extracting lipids from the media were different, being chloroform-ethanol (1:1), ethanol, and chloroform-ethanol (2:1). Extraction methods were applied to naked pDNA as the control. Four micrograms of naked pDNA and complexes including 4 μg of pDNA were incubated with 4 KU of DNase I for 10 min at 37 °C. Reactions were terminated by adding 40 μL of 25 mM EDTA solution.

3.9. Statistical analysis

Statistical evaluation of zeta potential values and particle sizes results of the formulations was achieved using the SPSS two-way ANOVA program.

4. Conclusion

SLNs containing DOTAP were prepared using an oil-in-water emulsification technique and characterized in vitro. The increase in zeta potentials correlated with the increase in the amount of DOTAP added to the formulations, which shows that solid lipid particles gained a cationic feature. Complex formation between DNA and SLNs occurred via electrostatic interactions. Positive charge on the particles caused efficient binding of DNA as demonstrated by gel retardation images. Only the zeta potentials of SLNs decreased after autoclave sterilization; particle sizes of SLNs did not show a significant increase ($P \geq 0.05$) under any tested conditions (4 °C, 25 °C, 40 °C). Appropriate storage conditions were determined to be 25 °C for lyophilized DSLN and 4 °C for lyophilized GSLN and CSLN. Among the SLN formulations studied, the most stable crystalline structure was found to be the lyophilized form. The results of the studies on the effect of production temperatures demonstrated a reduction in the efficacy of DOTAP depending on the increase in the heat exposed. Absence of the evidence of structural changes or abnormalities for mixtures of lipid matrices with DOTAP shows that DOTAP can be dissolved in the matrixes with no change in its structure. Conclusively, DOTAP-containing SLN systems seem to be promising gene delivery systems. However, further studies have to be performed to prove the efficiency of in vitro and in vivo transfection.

Acknowledgment

This study was supported by the Anadolu University Research Foundation (Project Number: 020315).

References

1. Parhiza, H.; Shierb, W. T.; Ramezani, M. *Int. J. Pharm.* **2013**, *457*, 237–259.
2. Ibraheem, D.; Elaissari, A.; Fessi, H. *Int. J. Pharm.* **2014**, *459*, 70–83.
3. Duvall, C. L.; Prokop A.; Gersbach, C. A.; Davidson, J. M. In *Principles of Tissue Engineering (Fourth Edition)*; Lanza, R.; Langer, R.; Vacanti, J. P., Eds. Elsevier: London, UK, 2014, pp. 687–723.

4. Büyükköroğlu, G.; Abbasoğlu, D.; Hızel, C. In *Omics Approaches in Breast Cancer; Towards Next-Generation Diagnosis, Prognosis and Therapy*; Barh, D., Ed. Springer: New Delhi, India, 2014, pp. 519–534.
5. Vighia, E.; Montanaria, M.; Hanuskovab, M.; Iannuccellia, V.; Coppia, G.; Leoa, E. *Int. J. Pharm.* **2013**, *440*, 161–169.
6. Worgall, S.; Crystal, R. G., Davidson, J. M. In *Principles of Tissue Engineering (Fourth Edition)*; Lanza, R.; Langer, R.; Vacanti, J. P., Eds. Elsevier: London, UK, 2014, pp. 657–686.
7. Moreta, I.; Peris, J. E.; Guillema, V. M.; Beneta, M.; Reverta, F.; Dasi, F.; Crespoa, A.; Alino, S. F. *J. Controlled Release* **2001**, *76*, 169–181.
8. Saccardo, P.; Villaverde, A.; González-Montalbán, N. *Biotechnol. Adv.* **2009**, *27*, 432–438.
9. Woodle, M.; Scaria, P. *Curr. Opin. Colloid Interface Sci.* **2001**, *6*, 78–84.
10. Tros de Ilarduya, C.; Sun, Y.; Düzgüneş, N. *Eur. J. Pharma. Sci.* **2010**, *40*, 159–170.
11. Zuidam, J. N.; Barenholz, Y. *Biochim. Biophys. Acta* **1998**, *1368*, 115–128.
12. Palmer, L. R.; Chen, T.; Lam, A. M. I.; Fenske, D. B.; Wong, K. F. *Biochim. Biophys. Acta* **2003**, *1611*, 204–216.
13. Olbrich, C.; Bakowsky, U.; Lehr, C. M.; Müller, R. H.; Kneuer, C. *J. Controlled Release* **2001**, *77*, 345–355.
14. Büyükköroğlu, G.; Yazan, Y.; Öner, F. In *Proceedings of 5th World Meeting on Pharmaceutics Biopharmaceutics and Pharmaceutical Technology*, Geneva, Switzerland, 27–30 March 2006, p. 41.
15. Joshi, M. D.; Müller, R. H. *Eur. J. Pharma. Biopharma.* **2009**, *71*, 161–172.
16. Radomska-Soukharev, A. *Adv. Drug Delivery Rev.* **2007**, *59*, 411–418.
17. Fàbregas, A.; Sánchez-Hernández, N.; Ticó, J. R.; García-Montoy, E.; Pérez-Lozano, P.; Suñé-Negre, J. M.; Hernández-Munain, C.; Suñé, C.; Miñarro, M. *Int. J. Pharm.* **2014**, *473*, 270–279.
18. Mehnert, W.; Mäder, K. *Adv. Drug Delivery Rev.* **2012**, *64*, 83–101.
19. Cortesi, R.; Campioni, M.; Ravani, L.; Drechsler, M.; Pinotti, M.; Esposito, E. *New Biotechol.* **2014**, *31*, 44–54.
20. Hou, D.; Xie, C. S.; Huang, K.; Zhu, C. H. *Biomaterials* **2003**, *24*, 1781–1785.
21. Cavalli, R.; Caputo, O.; Carlotti, M. E.; Trotta, M.; Scarnecchia, C.; Gasco, M. R. *Int. J. Pharm.* **1997**, *148*, 47–54.
22. Wissing, S. A.; Kayser, O.; Müller, R. H. *Adv. Drug Delivery Rev.* **2004**, *56*, 1257–1272.
23. Pardeike, J.; Weber, S.; Matsko, N.; Zimmer, A. *Int. J. Pharm.* **2012**, *439*, 22–27.
24. Kumar, S.; Randhawa, J. K. *Mater. Sci. Eng. C.* **2013**, *33*, 1842–1852.
25. Souto, E. B.; Wissing, S. A.; Barbosa, C. M.; Müller, R. H. *Eur. J. Pharma. Biopharma.* **2004**, *58*, 83–90.
26. Schwarz, C.; Mehnert, W.; Lucks, J. S.; Müller, R. H. *J. Controlled Release* **1994**, *30*, 83–96.
27. Bunjes, H.; Unruh, T. *Adv. Drug Delivery Rev.* **2007**, *59*, 379–402.
28. Jenning, V.; Thünemann, A. F.; Gohla, S. H. *Int. J. Pharm.* **2000**, *199*, 167–177.
29. Heurtault, B.; Saulnier, P.; Pech, B.; Proust, J. E. *Biomaterials* **2003**, *24*, 4283–4300.
30. Noack, A.; Hause, G.; Mädera, K. *Int. J. Pharm.* **2012**, *423*, 440–451.
31. Bunjes, H.; Koch, M. H. J. *J. Controlled Release* **2005**, *107*, 229–243.
32. Gaspar, V. M.; Correia, I. J.; Sousa, A.; Silva, F.; Paquete, C. M.; João, A.; Queiroz, A. J.; Sousa, F. *J. Controlled Release* **2011**, *156*, 212–222.
33. Huang, W.; Zhang, Z.; Han, X.; Tang, J.; Wang, J.; Dong, S.; Wang, E. *Bioelectrochemistry* **2003,** *59*, 21–27.
34. Mezei, A.; Pons, R.; Morán, M. C. *Colloids Surf. B Biointerfaces* **2013**, *111*, 663–671.
35. Mel'nikov, S. M.; Dias, R.; Mel'nikova, Y. S.; Marques, E. F.; Miguel, M. G.; Lindman, B. *FEBS Lett.* **1999**, *453*, 113–118.
36. Zuidam, N. J.; Barenholz, Y.; Minsky, A. *FEBS Lett.* **1999**, 457, 419–422.
37. An, H.; Jin, B. *Biotechnol. Adv.* **2012**, *30*, 1721–1732.
38. Büyükköroğlu, G.; Yazan, Y.; Öner, F. In *Proceedings of European Conference on Drug Delivery and Pharmaceutical Technology Symposium*, Seville, Spain, 2004, p. 133.